HortScience 52(12):1840–1848. 2017. doi: 10.21273/HORTSCI12229-17

Effects of Pigment Constituents and Their Distribution on Spathe Coloration of *Zantedeschia hybrida*

Ting Lei[1] and Yang Song[1]
Faculty of Modern Agricultural Engineering, Kunming University of Science and Technology, Kunmming 650500, China

Xuehua Jin[2], Tianyu Su, and Yiwen Pu
Faculty of Architecture and City Planning, Kunming University of Science and Technology, Kunming 650500, China

Additional index words. epidermal cells, stained cell layers, anthocyanins, flavonoids, black color mechanism

***Abstract*. The plant *Zantedeschia hybrida* is colorful and suitable for cut flowers and potted plants. This study employed a colorimetric method for the determination of spathe color phenotypes in 27 *Z. hybrida* cultivars and classified them into six major color classes. To characterize the coloration mechanism of the *Z. hybrida* spathe, this study explored the main colorants and pigment distribution using high-performance liquid chromatography (HPLC) with photodiode array detection (DAD) and electrospray ionization mass spectrometry (ESI-MS), ultra-performance liquid chromatography/hybrid triple quadrupole linear ion trap mass spectrometry (UPLC-Q-TRAP-MS), and tissue sections. The results showed that flavonoids were colorants in the spathes of different color groups and that cyanidin (Cy) was the main colorant, whereas carotenoids were not detected in the spathe. Total anthocyanin (TA) content was negatively correlated with lightness (*L**) of coloration, such that a spathe with a higher TA and thicker pigmented cell layer showed a deeper color; however, there was no correlation between deep coloration in a spathe and flattened upper epidermal cells. The difference in TA was the main reason for the color variation among *Z. hybrida* of different color groups, whereas the total flavones and flavonols (TF) played a key role in the coloration of the orange and yellow group.**

Flower colors are among the most adaptive phenotypes in plant evolutionary history; they provide an important basis for species classification and comprise a vital aspect of plant epigenetics (Deguchi et al., 2013; Sun et al., 2009). Flower coloration is affected by multiple factors such as pigment content and distribution in petals, the pH and metal ions of the pigmented cell sap, and petal epidermal cell structure (Dao et al., 2016; Jin et al., 2016; Li et al., 2014; Mol et al., 1998; Paech, 1955; Zhao et al., 2016). There are three main classes of pigments that contribute to flower color: flavonoids, carotenoids, and betalains (Griesbach, 2005). Anthocyanins are flavonoids that produce orange to blue–violet colors in flowers, whereas other flavonoids such as aurones and flavones render flowers light yellow or colorless (Mizuta et al., 2009; Zhao et al., 2004). Anthocyanins are generally distributed in epidermal cells, and the flower color is directly affected by the petal epidermal cell shape and pigment distribution (Kumi et al., 2009; Noda et al., 1994). In addition, palisade tissue and spongy tissue of petals with a deeper color also contain pigments (Yasuda, 1989a, 1989b). Petal epidermal cells usually have a conical shape and size that reflects light, thereby affecting the petal color by altering the light path (Zhang et al., 2016). The relationships among pigment composition and content, petal microstructure, and flower colors have been extensively studied, e.g., in moutan peony (*Paeonia suffruticosa*) (Wang et al., 2004; Zhang et al., 2007), lily (*Lilium* sp.) (Burchi et al., 2010; Yamagishi and Akagi, 2013; Yamagishi et al., 2014), and petunia (Burchi et al., 2010). However, few studies have been performed on *Z. hybrida*.

Zantedeschia hybrida is a native bulbous perennial herb of southern Africa that belongs to genus *Zantedschia* of the family *Araceae* (Singh et al., 1996). As a popular plant, it has attracted increasing interest in international floral markets because of its colorful and elegant appearance as well as its outstanding bouquet. Lewis et al. (2003) performed a preliminary study for *Z. hybrida* spathe phenotype determination and pigment analysis in 2003. However, because of the limitations of cultivar quantity and analytical technology, the mechanisms of spathe color formation are still currently unclear. Therefore, there is a need to collect more cultivars and use advanced technology to determine the composition and content of flavonoids and analyze the effects of microscopic structure on flower color, so as to further understand the mechanisms by which flower color is determined and to provide a basis for selection of superior parents to breed ideal colors at the same time.

In this study, we analyzed 27 *Z. hybrid* cultivars for their anthocyanin composition, content, and cross sections to resolve the relationship between the spathe color parameters of *Z. hybrida* and pigment composition and microstructure. Flower color phenotypes were defined and classified, and the metabolic pathway of anthocyanins in spathes was preliminarily deduced to provide a basis for understanding the coloration mechanism in spathes.

Materials and Methods

Plant materials. During a resource survey in Kunming area, the research group collected a total of 27 *Z. hybrida* cultivars (the main color groups in *Z. hybrida* were covered by all selected cultivars) mainly derived from the greenhouse of Kunming Trifecta orchid Nursery Co., Ltd. (lat. 24°33′N, long. 102°41′E), in May 2016. The cultivation conditions were as follows: 20 °C with a 12 h photoperiod provided by incandescent lights and humidity of 30% (constant temperature and humidity). Plants showing the same growth pattern were selected, and fully opened spathes were collected for flower color determination, slice preparation, and pigment analysis.

Color analysis. The colors of the fresh spathe of the 27 variants were first compared with the Royal Horticultural Society Color Chart, and the surface color of the spathe was analyzed with a Chroma Meter CR-400 [Konica Minolta (China) Investment Ltd., Shanghai, China] at *C*/2. Three spathe samples of each cultivar were taken from different plants. The *Z. hybrida* spathe was placed on clean white paper and the light source was aligned to the middle part of the spathe for measurement. Finally, using PASW Statistics 18 software, hierarchical clustering analysis was performed using phenotype values of spathe flower colors measured by colorimeter. The cluster analysis method using the furthest neighbor, coupled with CIElab color space data (Voss, 1992) was used to characterize spathe color.

Extraction of anthocyanins and TF. *Zantedeschia hybrida* spathes were quickly ground into fine powder in liquid nitrogen. After the liquid nitrogen was evaporated, 250 mg of spathe powder was added to 1 mL of anthocyanin extraction solution [V (methanol) : V (water) : V (formic acid) : V (trifluoroacetic acid) = 70:27:2:1]. Total flavones and flavonols were extracted from 100 mg of fresh sample with 1 mL of methanol as the extraction solution using

Received for publication 16 June 2017. Accepted for publication 23 Oct. 2017.
The work was supported by the National Natural Science Foundation of China (No. 31560568; No. 31760587).
[1]These authors contributed equally to this work.
[2]Corresponding author. E-mail: xh_kimlian@126.com.

Table 1. Spathe colors and color parameters of 27 *Z. hybrida* cultivars.

Color group and cultivars	RHSCC	CIELab coordinates				
		*L**	*a**	*b**	*C**	*h*°
Black group						
Mirages	N77A	19.20	4.94	0.18	4.96	2.06
Jack	N79A	22.53	9.53	0.03	9.53	0.02
Chocolate	187A	22.67	8.26	0.13	8.26	0.85
Cantor	N92A	23.89	5.56	–0.08	5.55	–0.82
Black Girl	N187	20.77	6.58	0.10	6.58	0.80
Prado	N92	24.39	16.50	–0.39	16.49	–1.35
Amaranth group						
Stanta Fe	64B	48.42	25.39	–1.00	25.39	–2.30
Lover	71B	36.69	40.12	–2.75	40.17	–3.80
Promise	22A	20.22	11.48	0.29	11.5	1.43
Picasso	79A	28.46	24.91	–6.37	25.58	–19.0
Premio	N34	51.94	–6.92	48.15	48.5	33.56
Red group						
Durance	44A	48.08	26.94	18.19	32.78	34.01
Figo	53D	31.99	45.46	13.53	47.57	16.65
Murano	53A	32.88	41.87	11.23	43.47	15.00
Trinity	N45	35.65	37.50	13.91	40.17	20.33
Yellow group						
Sun club	2B	73.59	–6.98	34.02	35.21	102
Solo	7A	81.22	–2.33	79.59	80.12	92
Jin cheng	6A	83.80	–6.38	71.30	72.08	96
Blanc	150D	74.15	–7.25	19.99	21.72	110
Pink group						
Romance	65B	71.37	7.76	3.17	8.57	22.19
Roseland	27B	80.50	4.41	10.73	12.05	67
Melrose	36B	69.51	7.94	7.04	10.93	41
Ventura	N155D	78.38	–1.36	6.63	7.24	102
Jian ai	55C	70.47	17.13	2.99	17.47	9.89
Orange group						
Phoenix	17B	74.22	5.1	79.36	80.02	86
Lido	N30D	58.89	14.01	27.76	31.53	63
Odean	32B	69.27	37.1	32.79	49.80	73.2

Note: *L** represents lightness, *a** represents redness, *b** represents yellowness, *C* represents chroma, $C = (a^{*2} + b^{*2})^{1/2}$, *h* represents hue angle, $h = \arctan(b^*/a^*)$ (Gonnet, 1993).
RHSCC = Royal Horticultural Society Color Chart.

the same processing method. Both extracts were incubated at 4 °C followed by a 24 h extraction, with vortexing every 12 h (Hashimoto et al., 2000; Jia et al., 2008; Yoshitama, 1981; Zhang et al., 2009). The extracts were filtered through a 0.2 µm filter to obtain the samples to be tested.

Measurement of TA and TF and their structural identification. Total anthocyanin was measured using HPLC (Li et al., 2008). TA was measured using an Agilent HPLC equipped with a P680 pump, UltiMate 3000 autosampler, DAD-100 ultraviolet-visible (ultraviolet-vis) detector, TCC-100 column oven and Agilent ZORBAX SB-Aq (4.6 mm × 250 mm) column. For the HPLC measurements, the mobile phase consisted of solvents A and B (solvent A : water : formic acid : trifluoroacetic acid = 97.9:2:0.1; solvent B : water : acetonitrile : formic acid : trifluoroacetic acid = 62.9:35:2:0.1). The mobile phase was subjected to ultrasonic degassing and 0.2 µm ultrafiltration before injection. The injection volume was 10 µL, the column temperature was 25 °C, and the flow rate was 0.8 mL·min^{-1}. The elution gradient profile of mobile phase B was 30% to 53% for 0–20 min, 53% to 53% for 20–40 min, 53% to 30% for 40–45 min, and 30% to 30% for 45–50 min. The peak areas of petal anthocyanin absorbance at a wavelength of 530 nm were determined (Jia et al., 2008).

For the HPLC-MS, HPLC-ESI-MS^n was used to analyze the structure of anthocyanins in typical samples using the Agilent 6540Q-TOT liquid chromatography–-mass spectrometry system. Liquid chromatography (LC) was performed based on the aforementioned conditions and procedures. Mass spectrometry (MS) conditions included ion trap analyzer scanning from m/z 100 to 1600; positive ionization mode with capillary voltage of 3500 V; nebulizer pressure of 200 kPa; capillary exit of 100 V; dry temperature of 350 °C; and drying gas (N_2) flow rate of 6.0 L·min^{-1} (Sun et al., 2010; Yamagishi et al., 2014). The mass spectra were analyzed using MZmine software (Okinawa Institute of Science and Technology, Okinawa, Japan).

TF was measured using an UPLC-Q-TRAP (Ultimate 3000-API 3200 Q TRAP) system (SCIEX, Redwood, CA) equipped with an MSLab HP-C18 (150 mm × 4.6 mm, 5 µm) column. For the UPLC measurements, the mobile phase consisted of solvent A (water) and solvent B (acetonitrile), an injection volume of 10 µL, column temperature of 50 °C, and flow rate of 1 mL·min^{-1}.

Petal TA and TF were calculated in µg·g^{-1} fresh petal using a semiquantitative method (compared with standards) (Wang et al., 2001). The content of each compound with standards was calculated using the external standard method (TA: $y = 0.00001x - 0.000$, $R^2 = 0.999$; TF: $y = 0.00005x - 0.09369$, $R^2 = 0.998$).

The anthocyanin quantitative standard was Cy, and the quantitative and qualitative standards for flavones and flavonols were naringenin, apigenin, luteolin, dihydromyricetin, dihydrokaempferol, dihydroquercetin, myricetin, kaempferol, and quercetin. The standards were purchased from Shanghai Yuanye Bio-Technology Co., Ltd. (Shanghai, China).

Extraction and measurement of carotenoids. *Zantedeschia hybrida* spathes (100 mg) were ground in liquid nitrogen and added to 5 mL of extraction solution [V (petroleum ether) : V (acetone) = 1:1] with thorough vortexing, followed by an 8 h overnight extraction in the dark (wrapped in aluminum foil) at 4 °C. The extract was then filtered and the filtrate was subjected to ultraviolet–visible spectroscopy at a wavelength range of 400–500 nm using a double-beam ultraviolet–visible spectrophotometer (TU-1901; Beijing Persee General Instrument Co., Ltd., Beijing, China) (Zhao et al., 2004).

Observation of the spathe cross section of Z. hybrida. The center regions of *Z. hybrida* where spathes maintain even coloration were used for the preparation of plant slices (Rasika et al., 2003). The center cross section of the spathes was manually cut using a shaver blade and placed on a slide for observation using a light microscope (Digital Sight DS-Fi2; Nikon Corporation, Tokyo Japan); photographs were taken using an attached camera.

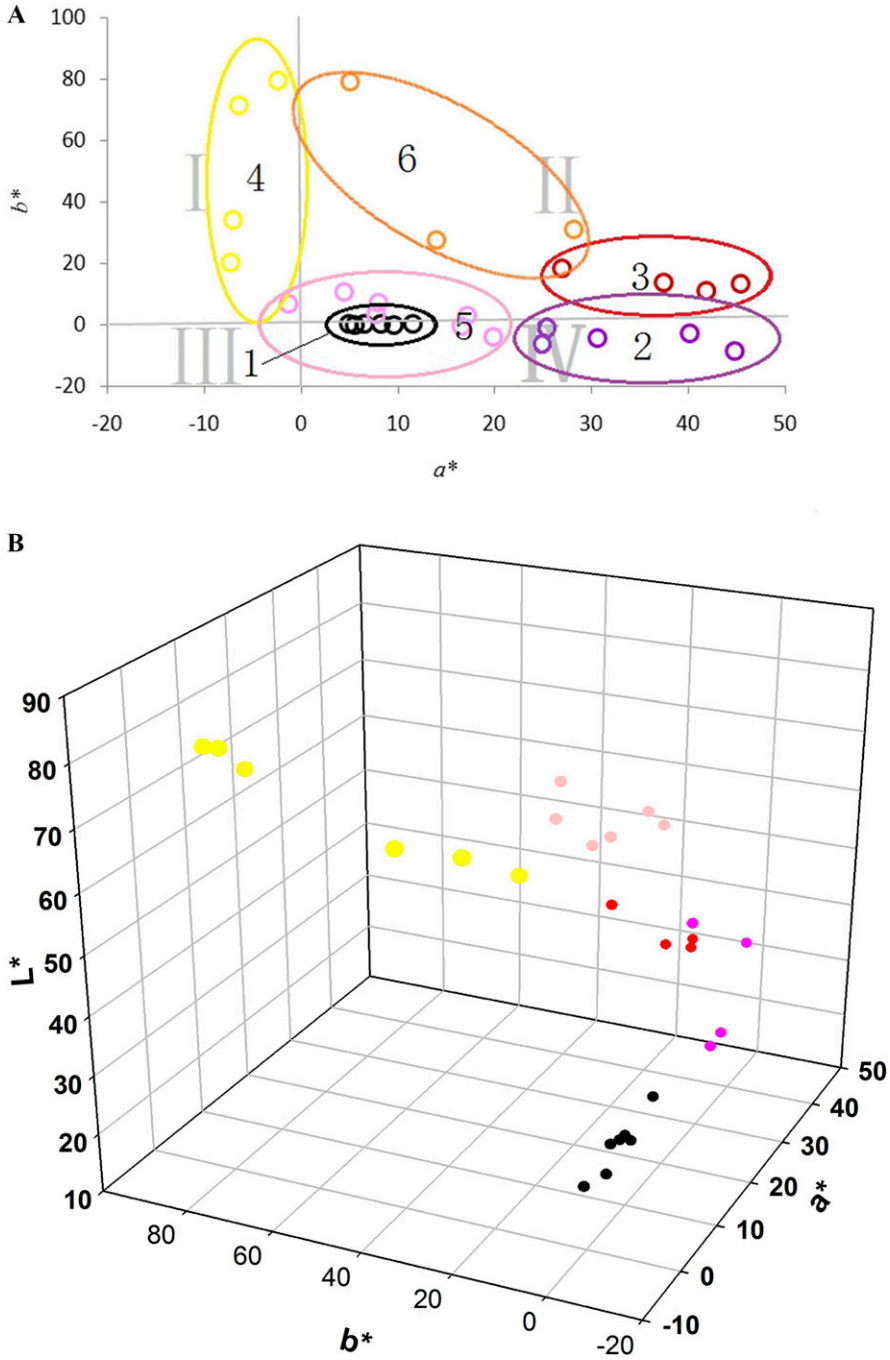

Fig. 1. Flower-color distribution of *Z. hybrida* cultivars in coordinate systems of bivariate (a^* and b^*) (**A**) and trivariate [lightness (L^*), a^*, and b^*] (**B**), respectively. 1: black group; 2: amaranth group; 3: red group; 4: yellow group; 5: pink group; 6: orange group.

Results

Analysis of the spathe color phenotypes of different Z. hybrida cultivars. The CIE L^*, redness (a^*), and yellowness (b^*) values of *Z. hybrida* spathes with different colors were measured using colorimetry and the data were subjected to cluster analysis. The flower colors were divided into six groups based on the transition line graphs plotted for black, amaranth, red, yellow, pink, and orange groups (Table 1).

The spathe colors of the 27 *Z. hybrida* cultivars were mainly distributed in Quadrants I, II, and IV on a^* and b^* hue coordinates, and no spathe color was distributed in Quadrant III of the blue area (Fig. 1A). The yellow group was distributed in Quadrant I, orange and red groups were distributed in Quadrant II, black and amaranth groups were mainly distributed in Quadrant IV, and the pink group was distributed in Quadrants I, II, and IV. The a^* values (redness) ranged from –7.25 (‘Blanc’) to 45.46 (‘Figo’); the b^* values (“yellowness”) ranged from –4.56 (‘Promise’) to 79.59 (‘Solo’); the h_{ab} (“hue angle”) ranged from –19° (‘Picasso’) to 110° (‘Blanc’).

The three-dimensional coordinate distribution of the L^*, a^*, and b^* values of the flower colors of each cultivar is shown in Fig. 1B. The L^* values of black, amaranth, and red groups were lower than those of the pink, yellow, and orange groups with a concentrated distribution. Among them, the black group had the lowest L^* value, whereas the pink and yellow groups had the highest L^* values. The L^* values ranged from 19.20 (‘Mirages’) to 83.80 (‘Solo’); the C values (chroma) ranged from 1.53 (‘Cantor’) to 80.02 (‘Solo’).

Different color groups of *Z. hybrida* have different relationships between L^* and C (Fig. 2). There was a significant positive relationship between C values and L^* values in the orange, yellow, and black groups (r^2 = 0.552, r^2 = 0.845, and r^2 = 0.546, respectively), where the L^* increased linearly with the increase in C. On the contrary, there was a significant negative correlation between the C value and the L^* values in the red group (r^2 = 0.904), where the L^* decreased linearly with the increase in C. No significant relationship was found for C values and L^* values in the amaranth and pink groups (r^2 = 0.0123, and r^2 = 0.228, respectively) (Supplemental Fig. 1).

Analysis of pigment composition and content in Z. hybrida spathe. Spathe anthocyanins in *Z. hybrida* were identified using HPLC-PAD to obtain the HPLC chromatogram of different color groups. The type of anthocyanin can be determined depending on the retention time of the anthocyanin peak (Yasuda, 1989a, 1989b). Two types of anthocyanins were detected from the results, namely A1 and A2, with retention times of 26 and 28 min, respectively. No anthocyanin absorption peak was detected in the yellow group or for ‘Ventura’ in the pink group (Fig. 3).

The mass spectra of anthocyanins showed that their molecular ions often carry a hydrogen ion and are present in the form of $[M + H]^+$. Anthocyanins were mainly classified based on the mass-to-charge ratio of glycoside ions $[Y_0]^+$ in their mass spectra (Beatriz et al., 2009; Cuyckens and Claeys, 2004; Stobiecki, 2000). In this study, we performed an MS analysis on these two types of anthocyanins (Supplemental Fig. 2). The molecular ions at m/z 595 $[(M + H)^+]$ were obtained from A1, which produced the characteristic fragment ions of Cy at m/z 287 $[(Y_0)^+]$ and other fragment ions at m/z 449. The molecular ions at m/z 595 $[(M + H)^+]$ were obtained from A2, which produced the characteristic fragment ions of pelargonidin (Pg) at m/z 271 $[(Y_0)^+]$ and of other fragment ions at m/z 433. Hence, it was inferred that A1 was Cy and that A2 was Pg. The common component in the spathe of all color groups, except for the yellow group, was A1 (Cy). It was also the main anthocyanin component in *Z. hybrida* spathes. By contrast, A2 (Pg) was mainly found in certain cultivars of red and orange groups (‘Murano’, ‘Trinity’, ‘Durance’, and ‘Lido’).

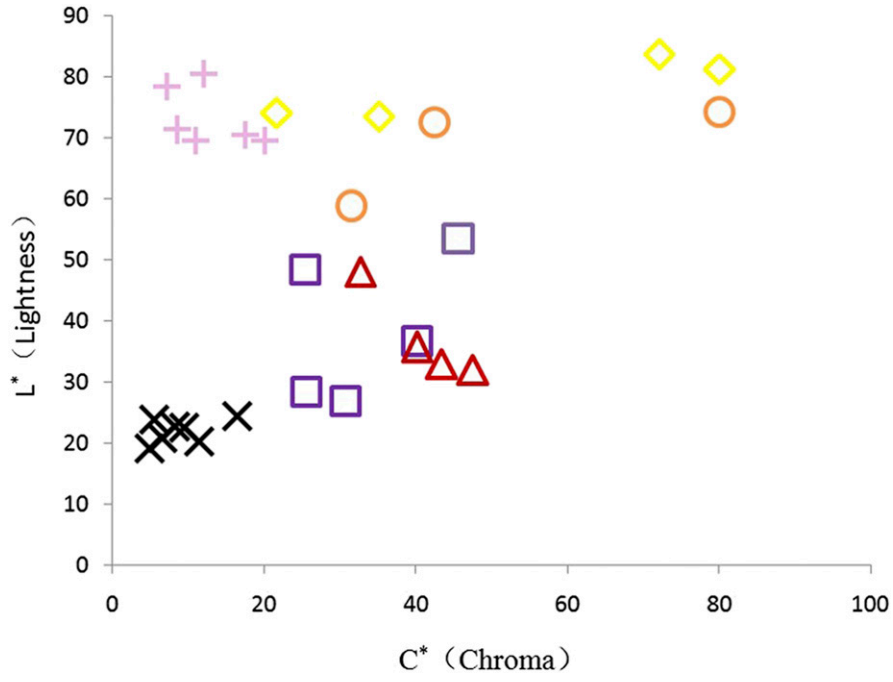

Fig. 2. Scatterplot based on lightness (L^*) and C values among *Z. hybrida* cultivars. ×: black group; □: amaranth group; Δ: red group; ◇: yellow group; +: pink group; ○: orange group.

The black group had a significantly higher spathe TA than the other color groups (Table 2; Fig. 4), followed by the amaranth, red, orange, and pink groups, and the TA content in each flower color group was highly significantly different ($P < 0.01$) (Table 3). 'Murano' had the highest proportion of Pg (38.5%) among four cultivars containing both Cy and Pg. All 27 cultivars were rich in TF with a copigmentation index (CI) that ranged from 8.12 to 989.06 (Table 2). The TF content in each flower color group was significantly different ($P < 0.05$) (Table 4).

UPLC-Q-TRAP-MS was used to analyze the composition of flavones and flavonols in the spathes of two cultivars ('Romance' and 'Black Girl'). Ten peaks from primary MS data were found to be associated with flavones and flavonols using comparison of standards. Comparison of the total ion chromatogram of spathe samples and standard total ion chromatogram (Supplemental Fig. 3) indicated that the samples from the two cultivars contained naringenin, luteolin, myricetin, dihydromyricetin, dihydrokaempferol, dihydroquercetin, kaempferol, quercetin, catechins, and epicatechin. Quantitative analysis using standards was performed (Table 5).

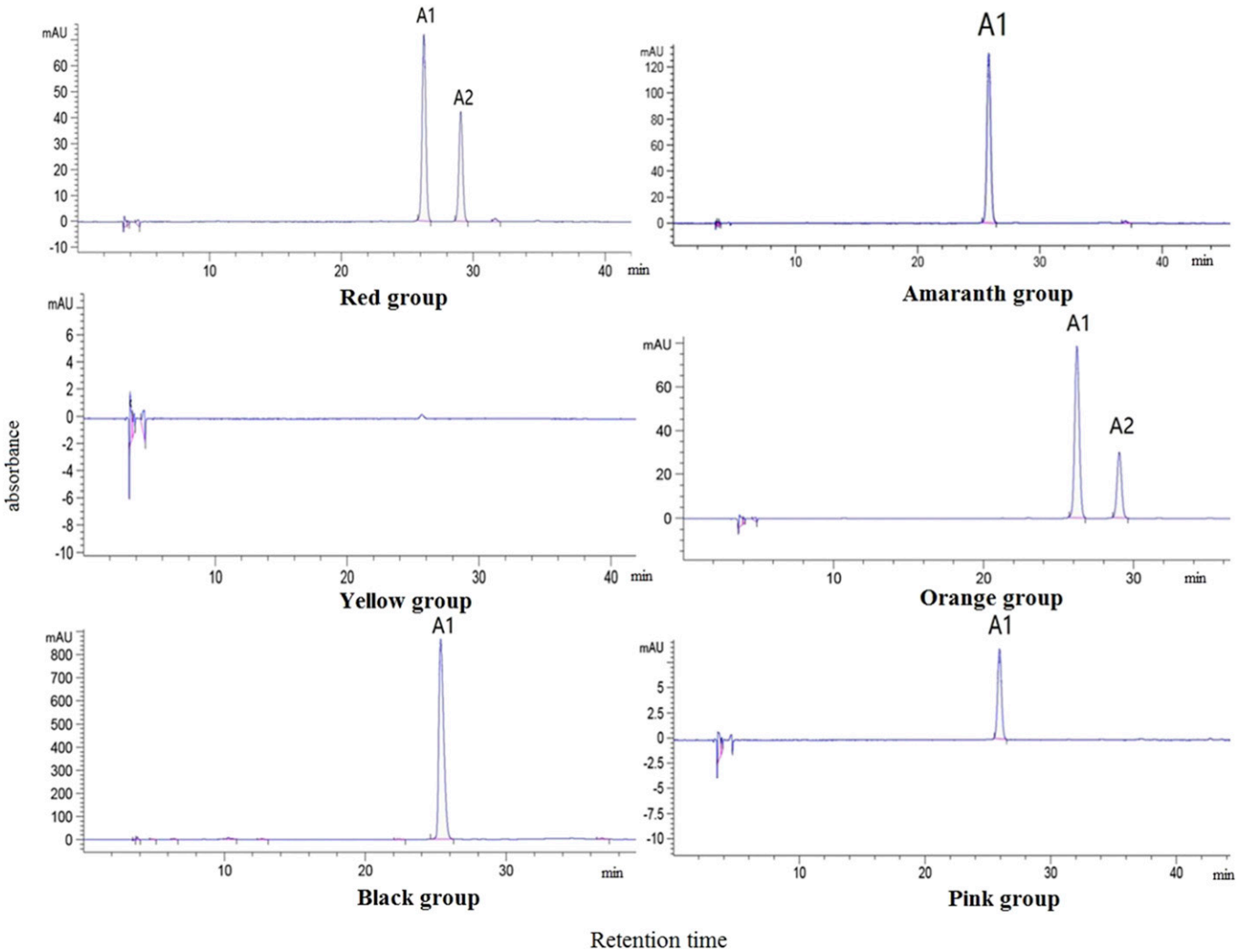

Fig. 3. The anthocyanin HPLC profiles of the main flower color in *Z. hybrid* (detected at 530 nm).

Table 2. Pigment constitutions and relative quantity of anthocyanins in 27 *Z. hybrida* cultivars.

Color group and cultivars[z]	Cy[y] (%)	Pg[y] (%)	TA[x] (μg·g^{-1})	TF[x] (μg·g^{-1})	CI[x]
1. Black group					
Mirages	100	—	485.1	7,249.6	14.9
Jack	100	—	617.2	8,362.0	13.5
Chocolate	100	—	546.0	7,013.3	12.8
Cantor	100	—	767.4	8,757.0	11.4
Black Girl	100	—	1,179.8	9,583.3	8.1
Prado	100	—	665.3	7,749.3	11.6
2. Amaranth group					
Stanta Fe	100	—	56.8	5,021.2	88.4
Lover	100	—	101.0	10,420.6	103.2
Promise	100	—	208.9	4,312.7	20.6
Picasso	100	—	100.3	3,775.3	37.3
Premio	100	—	164.0	4,668.6	28.5
3. Red group					
Durance	88	12.0	32.4	5,360.0	165.4
Figo	100	—	75.5	6,916.6	91.67
Murano	61.5	38.5	104.1	3,185.0	30.59
Trinity	83.1	16.9	78.7	4,243.4	53.91
4. Yellow group					
Sun club	—	—	—	5,589.9	∞
Solo	—	—	—	1,702.8	∞
Jin cheng	—	—	—	773.9	∞
Blanc	—	—	—	8,237.2	∞
5. Pink group					
Romance	100	—	14.3	4,548.6	319.0
Roseland	100	—	7.4	7,299.3	989.1
Melrose	100	—	5.7	1,086.2	189.6
Ventura	—	—	—	772.5	∞
Jian ai	100	—	20.8	4,450.8	214.0
6. Orange group					
Phoenix	100	—	5.8	4,457.4	768.5
Lido	71.5	28.5	74.2	4,312.7	58.1
Odean	100	—	65.1	4,201.0	64.5

[z]Cultivars were classified by anthocyanidins in the petals in association with petal coloration.
[y]Cy = cyanidin; Pg = pelargonidin. Data are expressed as percentage; — = not detected.
[x]TA = total anthocyanins; TF = total flavones and flavonols; CI = copigmentation index; CI = TF/TA. ∞: mean samples without glycosides of anthocyanin.

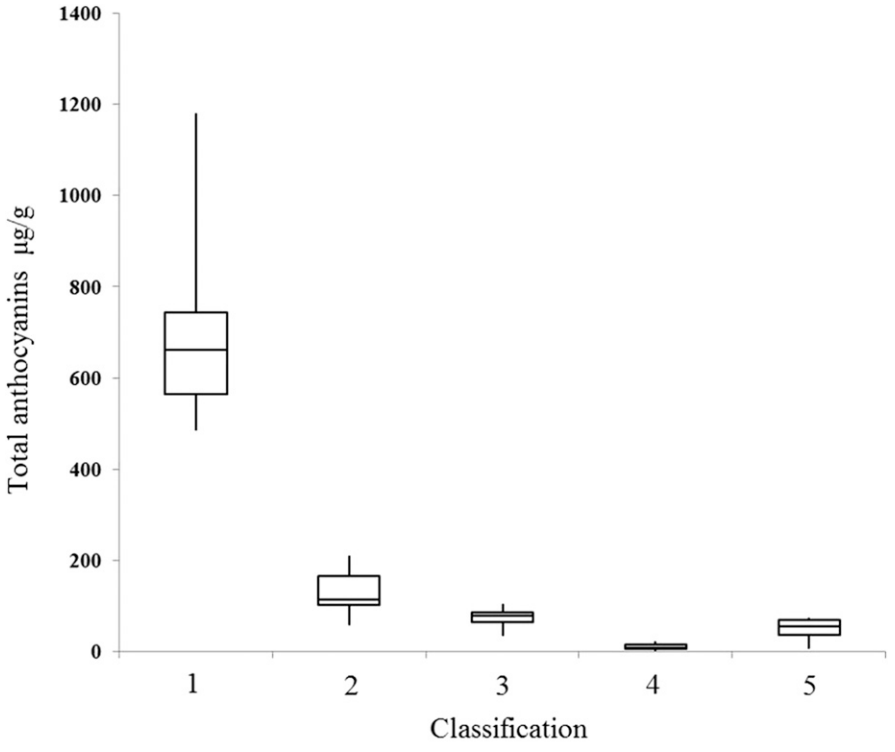

Fig. 4. Box plot of different color group of *Z. hybrid* cultivars based on total anthocyanins 1: black group; 2: amaranth group; 3: red group; 4: pink group; 5: orange group.

Measurement of the spathe carotenoid extract using ultraviolet–visible spectrometry indicated that none of the 27 *Z. hybrida* cultivars showed the characteristic absorption peak at wavelengths of 400–500 nm, indicating the absence of carotenoids in the *Z. hybrida* spathe.

Analysis of microstructure and pigment distribution in the Z. hybrida spathe. Analysis of the cross sections of the spathes of different *Z. hybrida* color groups showed that the spathe had flattened upper and lower epidermal cells, and that pigments were distributed in both upper and lower epidermal cells and mesophyll cells. In addition, spathes of different color groups had different numbers of stained cell layers, and spathes with a thicker stained cell layer had a deeper color (Fig. 5). Pigments of the black group were richly distributed in epidermal and mesophyll cells, and in the two to three layers of mesophyll cells close to both upper and lower epidermis. In the amaranth group, the pigments were distributed in the epidermal cells and the two layers of mesophyll cells; the lower epidermal cells and mesophyll cells close to the lower epidermis presented reduced accumulation compared with the upper epidermal cells. In the red and orange groups, pigments were distributed in the epidermal cells and a single layer of mesophyll cells. In the pink group, pigments were present only in the epidermal cells. Anthocyanins were not found in the yellow group or in 'Ventura' of the pink group. Thus, spathe coloration in *Z. hybrida* was closely associated with pigment distribution in the spathe.

Discussion

Correlation among spathe color parameters in Z. hybrida. This study performed a hierarchical

Table 3. The analysis of variance analysis of the content of total anthocyanin among six flower color group of *Z. hybrida.*

Variation source	SS	DF	MSS	*F*	$F_{0.01}$
Among class	1,909,120.7	5	381,824.14	29.73	4.042
Inner class	269,711.4	21	12,843.4		
Total	2,178,832.1	26			

SS = square sum; DF = degree of freedom; MSS = mean square sum; *F* = mean square sum among class/mean square sum inner class; $F_{0.01}$ = the threshold value of *F* at 0.01.

Table 4. The analysis of variance analysis of the content of TF among six flower color group of *Z. hybrida.*

Variation source	SS	DF	MSS	*F*	$F_{0.01}$
Among class	65,306,474.59	5	13,061,294.8	2.74	2.68
Inner class	100,129,569.60	21	4,768,074.71		
Total	165,436,044.20	26			

SS = square sum; DF = degree of freedom; MSS = mean square sum; *F* = mean square sum among class/mean square sum inner class; $F_{0.01}$ = the threshold value of *F* at 0.01.

Table 5. The composition and content of flavones and flavonols in 'Black girl' and 'Romance'.

Cultivars flavonoids ($\mu g \cdot g^{-1}$)	Romance	Black girl
Naringenin	0.80	4.60
Luteolin	3.0	0.0
Myricetin	75.7	41.2
Dihydromyricetin	48.9	495.0
Dihydrokaempferol	234.0	1,370.0
Dihydroquercetin	17.2	40.4
Kaempferol	1,660.0	2,540.0
Quercetin	21.9	163.0
Catechin	255.0	1,070.0
Epicatechin	351.0	5,320.0

analysis of flower color phenotypes *L**, *a**, and *b**, and established a measurement system for defining and classifying the flower color of *Z. hybrida*. The 27 collected cultivars were classified into six major color systems. When drawing the various color systems of *Z. hybrida* on the two-dimensional hue a, b coordinate scatter plot, we found that the yellow-color group was mainly distributed at 90 degrees around the coordinates, whereas the red-, black-, pink-, and amaranth-color groups were distributed at zero degrees around the coordinates, and the orange-color group was distributed at the second quadrant of the coordinates. This is generally consistent with the definition and distribution of colors in the CIElab color space (Voss, 1992), proving that the definition and classification of *Z. hybrida* flower colors in this study are scientific and reasonable.

Different *Z. hybrida* color groups had different relationships between *L** and *C*. *L** values and *C* values of orange and yellow groups had a significant positive relationship, whereas the red group had a significant negative relationship. The linear regressions in the black, amaranth, and pink groups were nonsignificant. In previous studies, some color groups of *Chrysanthemum morifolium* cultivars (Hong et al., 2012) and some color groups of *Consolida ajacis* cultivars (Hashimoto et al., 2000) showed a significant negative relationship with the *L** and *C* values. The differences in the correlation between *L** and *C* values may be due to differences in anthocyanin compositions and distribution, as well as different petal cross-sectional structures in different cultivars.

Relationship between the main pigments and phenotypes in Z. hybrida. The flower color is an important ornamental trait of plants (Nielsen et al., 2003). This study identified spathe anthocyanins in 27 *Z. hybrida* cultivars and found that the yellow group and 'Ventura' of the white group did not contain anthocyanins. Cultivars of all other color groups contained anthocyanins with Cy as the main component, whereas Pg only accumulated in four cultivars. Cy produced varying degrees of amaranth coloration of the spathe, similar results have been obtained in previous studies (He et al., 2011), whereas Pg produced varying degrees of vermilion color. According to a study of *Papaver nudicaule*, Pg is also an important coloring material that makes the petals red and orange (Bettina et al., 2016). The flavonoid composition of typical *Araceae* plants is relatively simple (Williams et al., 1981); for the *Z. hybrida* cultivars tested in this study, there was only one anthocyanin in 18 cultivars, and only two anthocyanins were found in the four cultivars. Anthocyanin was not detected in other cultivars, and carotenoids were not detected in any cultivars. Therefore, we believe that TF was the main pigment type producing yellow and orange colors. However, Lewis et al. (2003) found accumulation of carotenoids in cultivars of yellow and orange groups, possibly as the result of differences among cultivars. Flavones and flavonols are important copigments that exert their copigmentation effects when the CI exceeds 5 (Asen et al., 1971). In this study, the CI values of all tested cultivars were greater than 5, indicating that flavones and flavonols play a relatively greater role in the coloration of *Z. hybrida.*

Previous studies have demonstrated that petal anthocyanins affect light absorption (Hughes et al., 2006; Merzlyak et al., 2008). The study of the relationship between the spathe phenotype and TA in *Z. hybrida* revealed a significant negative relationship between TA and *L** value (r^2 = 0.615) (Fig. 6), i.e., large amounts of TA decreased the *L** values. The pink (r^2 = 0.849), red (r^2 = 0.667), and orange (r^2 =0.511) (Supplemental Fig. 4) color groups showed significant positive relationship between *a** value and TA, demonstrating that TA content in these color groups is closely associated with redness. The *b** value and TF value and the orange-color group showed a significant positive relationship (r^2 = 0.766) (Supplemental Fig. 4), suggesting that the formation of the orange-color group resulted from the combined effects of TA and TF. In previous studies on *Z. hybrida* (Lewis et al., 2003), the test materials were relatively uniform (orange, red, and pink color groups), and the *L** values were distributed from 28.4 to 89.5, the *h* values were distributed from 35° to 359°, and the TA concentration was ≈0–24 $\mu g \cdot g^{-1}$. In the test materials in this study, the *L** values were distributed around 19.2–83.8, *h* values were ≈0.2° to 110°, and TA content was ≈0–1179.8 $\mu g \cdot g^{-1}$, which basically covered all existing major *Z. hybrida* color groups and cultivars and meant that we systematically analyzed the relationship between the type and content of anthocyanins and flower color phenotypes.

Black color in flowers is a highly attractive trait in the floricultural industry. Flower color shows species specificity and black flowers in different species have different coloring mechanisms. Dahlia flowers are presented as black generally because of low *L** and low *C* (Deguchi et al., 2013, 2015). The black cultivars collected in our study also have low *L** and *C* values. The petals of black Dahlia cultivars accumulated large amounts of anthocyanins (Deguchi et al., 2013). Similarly, the black cultivars in our study also showed the largest accumulation of anthocyanin content (1179.8 $\mu g \cdot g^{-1}$). In addition, TA content in the spathes of 27 cultivars showed a significant negative relationship with *L** values, i.e., when *L** values were reduced to present a black phenotype, TA was an important factor. The main reason for black *Alcea rosea* 'Nigra' presenting as a black flower is the copigmentation of flavonols and flavones and accumulation of large amounts of anthocyanins (Hosaka et al., 2012). In the six black cultivars collected in this study, in addition to extensive accumulation of anthocyanins, flavonols and flavones accumulated in large amounts at the same time, and copigmentation may thus play some role in black coloration.

To further analyze the causes of the formation of the black group, this study compared the intermediate metabolites of flavonoids in 'Black Girl' of the black group and 'Romance' of the pink group, and characterized the metabolic pathway of anthocyanins in both cultivars (Fig. 7A and B). The amount of intermediate metabolites in both cultivars varied greatly (Table 5), with significantly higher amounts in 'Black Girl' than in 'Romance'. In addition, 'Black Girl' cultivars did not accumulate flavones,

Fig. 5. Images of *Z. hybrida* cultivars of each color group and their cross-sectional structures. 1: black group; 2: amaranth group; 3: red group; 4: yellow group; 5: pink group; 6: orange group. a: 'Mirages'; b: 'Jack'; c: 'Chocolate'; d: 'Cantor'; e: 'Black girl'; f: 'Prado'; g: 'Stanta Fe'; h: 'Lover'; i: 'Promise'; j: 'Picasso'; k: 'Premio'; l: 'Durance'; m: 'Figo'; n: 'Murano'; o: 'Trinity'; p: 'Sun Club'; q: 'Solo'; r: 'Jin cheng'; s: 'Blanc'; t: 'Romance'; u: 'Roseland'; v: 'Melrose'; w: 'Ventura'; x: 'Jian ai'; y: 'Phoenix'; z: 'Lido'; α: 'Odean'.

possibly because of the inhibition of *FNS* expression in 'Black Girl' that leads to inhibition of flavone synthesis as a result of competition with anthocyanins synthesis, thereby resulting in high accumulation of anthocyanins. This result was similar to that previously reported in Dahlia (Deguchi et al., 2013). Dihydromyricetin and myricetin were detected in both cultivars, which suggests that F3′5′H may exist in *Z. hybrida*. However, these plants were incapable of accumulating delphinin to produce a blue coloration. This result requires further study.

Relationship between colorant distribution in the Z. hybrida spathe and phenotype. When light shines on the petals to penetrate the pigment layer, a higher number of pigment layers lead to higher light absorption and the proportion of incident light entering the cells increases, resulting in a deeper flower color (Gorton and Vogelmann, 1996; Noda et al., 1994; Rasika et al., 2003). It was found in this study that colorants were distributed in the upper and lower epidermal cells, as well as in multiple layers of mesophyll cells near the epidermal cells (palisade and spongy tissues) of the *Z. hybrida* spathe. In addition, cultivars of different color groups had different numbers of pigmented cell layers; a spathe with a thicker pigmented layer had a deeper color and the black group had the thickest pigmented cell layer. This is similar to the effects of pigment distribution in grape hyacinth on coloring (Qi et al., 2013). Cross-sectional structural observation indicated that the flavones and flavonols that cause yellow flower coloration are mainly distributed in the mesophyll cells of spathes, which is a different cell layer from where anthocyanins are distributed. This resulted in a background effect, particularly in orange coloration of spathes.

The shape of the petal epidermal cells affects the optical properties of the anthocyanin they contain, thereby affecting the appearance of the petals. Most angiosperms have conical petal upper epidermal cells that enhance the proportion of incident light entering the epidermal cells and the light absorption by pigments, thereby increasing the color intensity of the flower (Baumann et al., 2007). However, analysis of the microstructure of the spathes of the 27 cultivars examined in this study indicated that their epidermal cells did not have a conical shape, but rather a flattened shape, which resulted in greater light reflection that reduced the color intensity of the flowers (Gorton and Vogelmann, 1996). Therefore, the shape of the spathe epidermal cells was unrelated to the formation of the black *Z. hybrida* group. Conical epidermal cells can enhance color saturation (Baumann et al., 2007), whereas the flattened spathe epidermal cells of *Z. hybrida* reduce color saturation, which may be the main reason for the absence of correlation among *C* value, TA, and TF in this study.

In conclusion, the coloration of the *Z. hybrida* spathe is closely associated with its pigment components and contents as well as the cross-sectional structure of the spathe. The formation of the *Z. hybrida* spathe in the

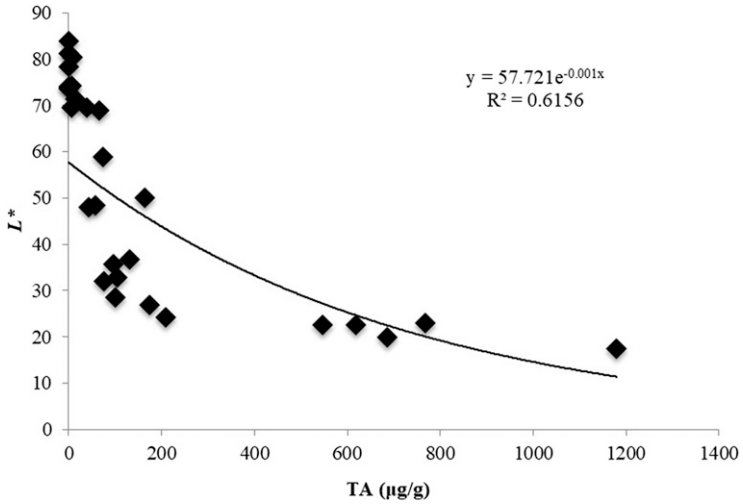

Fig. 6. Relationship between L^* and total anthocyanins (TA) in *Z. hybrida* cultivars of different color groups.

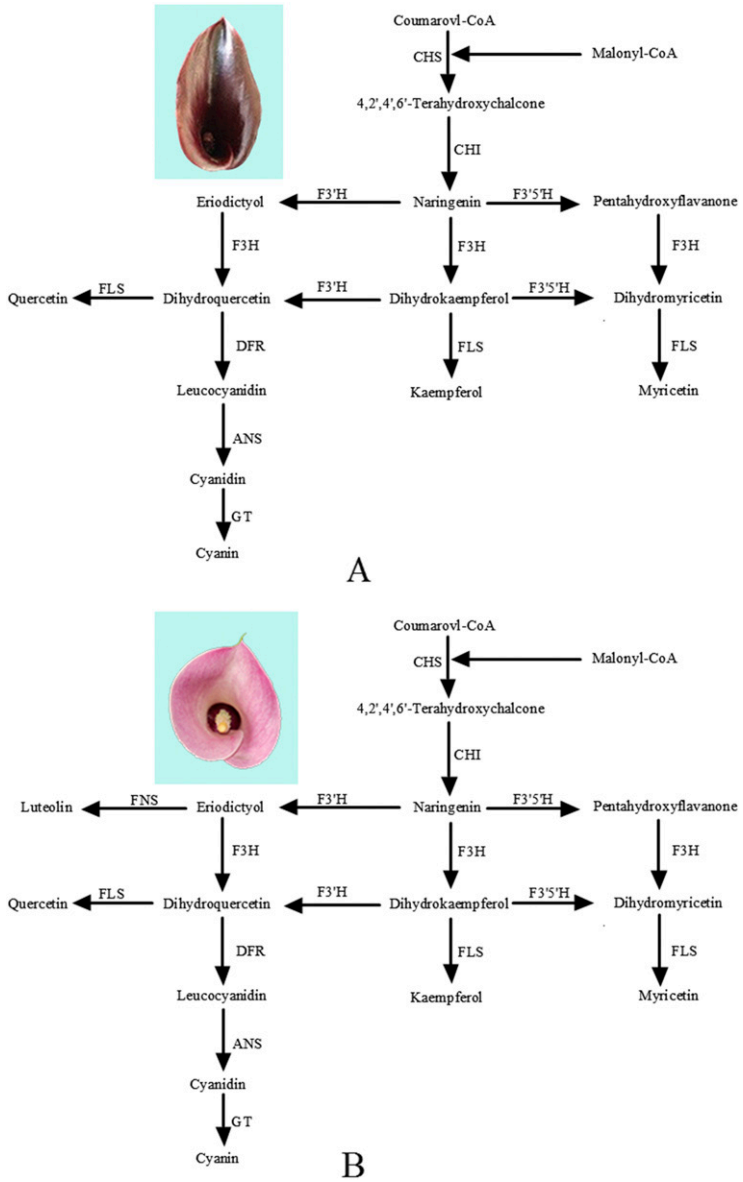

Fig. 7. Inferred metabolic pathways of anthocyanins in *Z. hybrida* spathe. (**A**) 'Black girl'; (**B**) 'Romance'.

black group was closely associated with high TA and accumulation of anthocyanins in multiple cell layers, and was not correlated with the shape of epidermal cells. Analysis of the relationship between the coloration of *Z. hybrida* and its pigment compositions, contents, and distribution is important for resolving the coloration mechanism of the *Z. hybrida* spathe and for molecular breeding to improve the color of the flowers.

Literature Cited

Asen, S., R.N. Stewart, and K.H. Norris. 1971. Co-pigmentation effect of quercetin glycosides on 304 absorption characteristics of cyanidin glycosides and color of Red Wing Azalea. Phytochemistry 10(1):171–175.

Baumann, K., R.M. Perez, D. Bradley, J. Venail, P. Bailey, H. Jin, R. Koes, K. Roberts, and C. Martin. 2007. Control of cell and petal morphogenesis by R2R3 myb transcription factors. Development 134(9):1691–1701.

Beatriz, A.G., L.A. Berrueta, S. Garmón-Lobato, B. Gallo, and F. Vicente. 2009. A general analytical strategy for the characterization of phenolic compounds in fruit juices by high-performance liquid chromatography with diode array detection coupled to electrospray ionization and triple quadrupole mass spectrometry. J. Chromatogr. A 1216(28):5398–5415.

Bettina, D., A.C. Warskulat, and B. Schneider. 2016. The occurrence of flavonoids and related compounds in flower sections of *Papaver nudicaule*. Plants 5(2):28.

Burchi, G., D. Prisa, A. Ballarin, and P. Menesatti. 2010. Improvement of flower color by means of leaf treatments in lily. Scientia Hort. 125(3): 456–460.

Cuyckens, F. and M. Claeys. 2004. Mass spectrometry in the structural analysis of flavonoids. J. Mass Spectrom. 39(1):1–15.

Dao, T.T.H., K. Ureshino, D.T. Van, and I. Miyajima. 2016. Co-pigmentation of anthocyanin-flavonol in the blotch area of *Rhododendron simsii* planch flowers. Jpn. Soc. Hort. Sci. 85(3):232–237.

Deguchi, A., S. Ohno, M. Hosokawa, F. Tatsuzawa, and M. Doi. 2013. Endogenous post-transcriptional gene silencing of flavone synthase resulting in high accumulation of anthocyanins in black dahlia cultivars. Planta 237:1325–1335.

Deguchi, A., F. Tatsuzawa, M. Hosokawa, M. Doi, and S. Ohno. 2015. Tobacco streak virus (strain dahlia) suppresses post-transcriptional gene silencing of flavone synthase II in black dahlia cultivars and causes a drastic flower color change. Planta 242(3):663–675.

Gonnet, J.F. 1993. CIElab measurementa precies communication in flower color: An example with carnation (*Dianthus caryophyllus*) cultivars. J. Hort. Sci. 68(4):499–510.

Gorton, H.L. and T.C. Vogelmann. 1996. Effects of epidermal cell shape and pigmentation on optical properties of *Antirrhinum* petals at visible and ultraviolet wavelengths. Plant Physiol. 112:879–888.

Griesbach, R.J. 2005. Biochemistry and genetics of flower color. Plant Breed. Rev. 25:89–114.

Hashimoto, F., M. Tanaka, H. Maeda, K. Shimizu, and Y. Sakata. 2000. Characterization of cyanic flower color of *Delphinium* cultivars. J. Jpn. Soc. Hort. Sci. 69(4):428–434.

He, Q.L., Y. Shen, M.X. Wang, M.R. Huang, R.Z. Yang, S.J. Zhu, L.S. Wang, Y.J. Xu, and R.L. Wu. 2011. Natural variation in petal color in *Lycoris longituba* revealed by anthocyanin components. PLoS One 6(8):e22098.

Hong, Y., X.X. Bai, W. Sun, F.W. Jia, and S.L. Dai. 2012. The numerical classification of *Chrysanthemum* flower color phenotype. Acta Hort. Sin. 39(7):1330–1340. (in Chinese).

Hosaka, H., T. Mizuno, and T. Iwashina. 2012. Flavonoid pigments and color expression in the flowers of black *Hollyhock* (Alcea rosea 'nigra'). Bull. Natl. Mus. Nat. Sci. 38:69–75.

Hughes, N.M., H.S. Neufeld, and K.O. Burkey. 2006. Functional role anthocyanins in high-light winter leaves of the evergreen herb *Galax urceolata*. New Phytol. 168:575–587.

Jia, N., Q.Y. Shu, L.S. Wang, H. Du, Y.J. Xu, and Z.A. Liu. 2008. Analysis of petal anthocyanins to investigate coloration mechanism in herbaceous peony cultivars. Scientia Hort. 117:167–173.

Jin, X.H., H. Huang, L. Wang, Y. Sun, and S.L. Dai. 2016. Transcriptomics and metabolite analysis reveals the molecular mechanism of anthocyanin biosynthesis branch pathway in different *Senecio cruentus* cultivars. Front. Plant Sci. 7(107):1307.

Kumi, Y., M. Mihoko, and K. Tadao. 2009. Blue flower color development by anthocyanins: From chemical structure to cell physiology. Nat. Prod. Rep. 26(7):884–915.

Lewis, D.H., H.S. Arathoon, E.E. Swinny, S.C. Huang, and K.A. Funnell. 2003. Anthocyanin and carotenoid pigments in spathe tissue from selected *Zantedeschia* hybrids. Acta Hort. 624:147–154.

Li, C.H., L.S. Wang, Q.Y. Shu, Y.J. Xu, and J. Zhang. 2008. Pigments composition of petals and floral color change during the blooming period in *Rhododendron mucronulatum*. Acta Hort. Sin. 35(7):1023–1030.

Li, Q., J. Wang, H.Y. Sun, and X. Shang. 2014. Flower color patterning in pansy (*Viola* ×*wittrockiana* Gams) is caused by the differential expression of three genes from the anthocyanin pathway in acyanic and cyanic flower areas. Plant Physiol. Biochem. 84:134–141.

Merzlyak, M.N., O.B. Chivkunova, A.E. Solovchenko, and K.R. Naqvi. 2008. Light absorption by anthocyanins in juvenile, stressed, and senescing leaves. J. Expt. Bot. 59(14):3903–3911.

Mizuta, D., T. Ban, I. Miyajima, A. Nakatsuka, and N. Kobayashi. 2009. Comparison of flower color with anthocyanin composition patterns in evergreen Azalea. Scientia Hort. 122(4): 594–602.

Mol, J., E. Grotewold, and R. Koes. 1998. How genes paint flowers and seeds. Trends Plant Sci. 3:212–217.

Nielsen, K.M., D.H. Lewis, and E.R. Morgan. 2003. Characterization of carotenoid pigments and their biosynthesis in two yellow flowered lines of *Sandersonia aurantiaca* (Hook). Euphytica 130(1):25–34.

Noda, K., B. Glover, P. Linstead, and C. Martin. 1994. Flower colour intensity depends on specialized cell shape controlled by a Myb-related transcription factor. Nature 369:661–664.

Paech, K. 1955. Colour development in flowers. Organization 12(6):401–435.

Qi, Y., L. Qian, H. Li, J. Yue, Y. Liu, and Y. Wang. 2013. Anatomical and biochemical studies of bicolored flower development in *Muscari latifolium*. Protoplasma 250(6):1273–1281.

Rasika, G.M., R.K. Adelheid, and D.A. Teresita. 2003. Pigment distribution and epidermal cell shape in *Dendrobium* species and hybrids. HortScience 38:573–577.

Singh, Y., A.E.V. Wyk, and H. Baijnath. 1996. Floral biology of *Zantedeschia aethiopica* (L). spreng. (*Araceae*). S. Afr. J. Bot. 62(3):146–150.

Stobiecki, M. 2000. Application of mass spectrometry for identification and structural studies of flavonoid glycosides. Phytochemistry 54(3): 237–256.

Sun, W., C.H. Li, L.S. Wang, and S.L. Dai. 2010. Accumulation and variation of anthocyanins in blue flowers of *Senecio cruentus* at different flowering stages. Beijing Fore Univ. 35(7): 1023–1030.

Sun, W., C.H. Li, L.S. Wang, S.L. Dai, and Y.J. Xu. 2009. Anthocyanins present in flowers of *Senecio cruentus* with different colors. Acta Hort. Sin. 36:1775–1782.

Voss, D.H. 1992. Relating colorimeter measurement of plant color to the royal horticultural society colour chart. HortScience 27:1256–1260.

Wang, L.S., F. Hashimoto, A. Shiraishi, N. Aoki, J.J. Li, and Y. Sakata. 2004. Chemical taxonomy of the xibei Tree peony from china by floral pigmentation. J. Expt. Bot. 117:47–55.

Wang, L.S., A. Shiraishi, F. Hashimoto, N. Aoki, K. Shimizu, and Y. Sakata. 2001. Analysis of petal anthocyanins to investigate flower coloration of zhongyuan (chinese) and daikon island (japanese) tree peony cultivars. J. Expt. Bot. 114:33–43.

Williams, C.A., J.B. Harborne, and S.J. Mayo. 1981. Anthocyanin pigments and leaf flavonoids in the family *Araceae*. Phytochemistry 20:217–234.

Yamagishi, M. and K. Akagi. 2013. Morphology and heredity of tepal spots in asiatic and Oriental lilies (*Lilium* spp.). Euphytica 194(3): 325–334.

Yamagishi, M., H. Ihara, K. Arakawa, S. Toda, and K. Suzuki. 2014. The origin of the lhmyb12, gene which regulates anthocyanin pigmentation of tepals, in Oriental and Asiatic hybrid lilies (*Lilium* spp.). Scientia Hort. 174(1):119–125.

Yasuda, Q. 1989a. In: Y.L. Fu (ed.). Flower color physiology biochemistry, p. 9–51. Trans. China For. Publ. House, Beijing, China.

Yasuda, Q. 1989b. In: Zhan and Z.C. Tong (eds.). The mystery of flower color, p. 31–50. Trans. China For. Publ. House, Beijing, China.

Yoshitama, K. 1981. Caffeic acid 4-β-glucoside as the acyl moiety of the *Senecio cruentus*, anthocyanin. Phytochemistry 20(1):186–187.

Zhang, J.J., L.S. Wang, Q.Y. Shu, Z.A. Liu, C.H. Li, J. Zhang, X.L. Wei, and D.K. Tian. 2007. Comparison of anthocyanins in non-blotches and blotches of the petals of xibei tree peony. Scientia Hort. 114(2):104–111.

Zhang, J.L., D.R. Pan, Y.F. Zhou, Z.C. Wang, S.M. Hua, L.L. Hou, and F.F. Sui. 2009. Cloning and expression of genes involved in anthocyanins synthesis in ornamental sunflower. Acta Scientia Hort. 36(1):73–80.

Zhang, Y., J.Y. Wu, Y.N. Wu, M.W. Tang, and L.N. Xie. 2016. Progresses and perspective of the function of MYB transcription factor MIXTA and its *Orthologous* gene. Scientia Agr. Sin. 49(7):1230–1241.

Zhao, C., W. Guo, and J. Chen. 2004. Preliminary study on the categories and contents of the flower color pigments of *Prunus mume* sieb et zucc. J. Beijing For. Univ. 26(2):68–73.

Zhao, D.Q., M.R. Wei, D. Liu, and J. Tao. 2016. Anatomical and biochemical analysis reveal the role of anthocyanins in flower coloration of herbaceous peony. Plant Physiol. Biochem. 102:97–106.

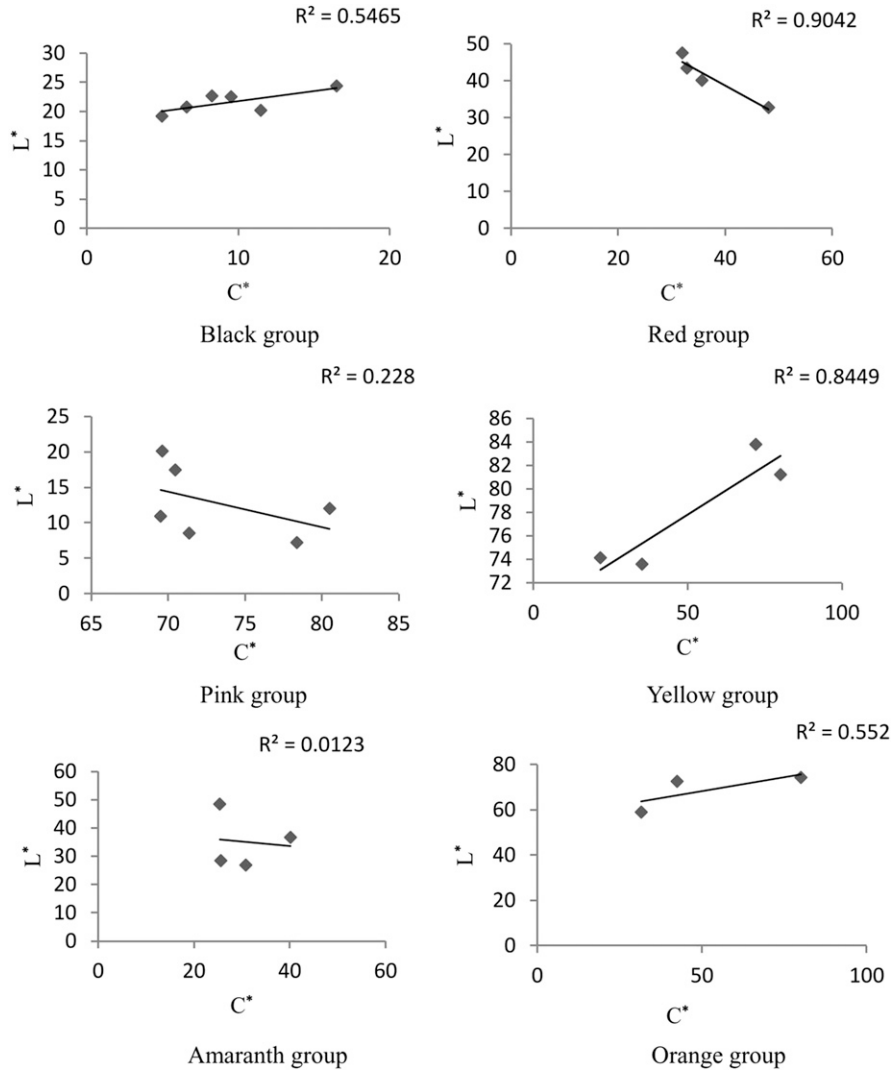

Supplemental Fig. 1. Relationships between redness (or yellowness) and total anthocyanin (or total flavones and flavonols) of *Z. hybrida* each color group.

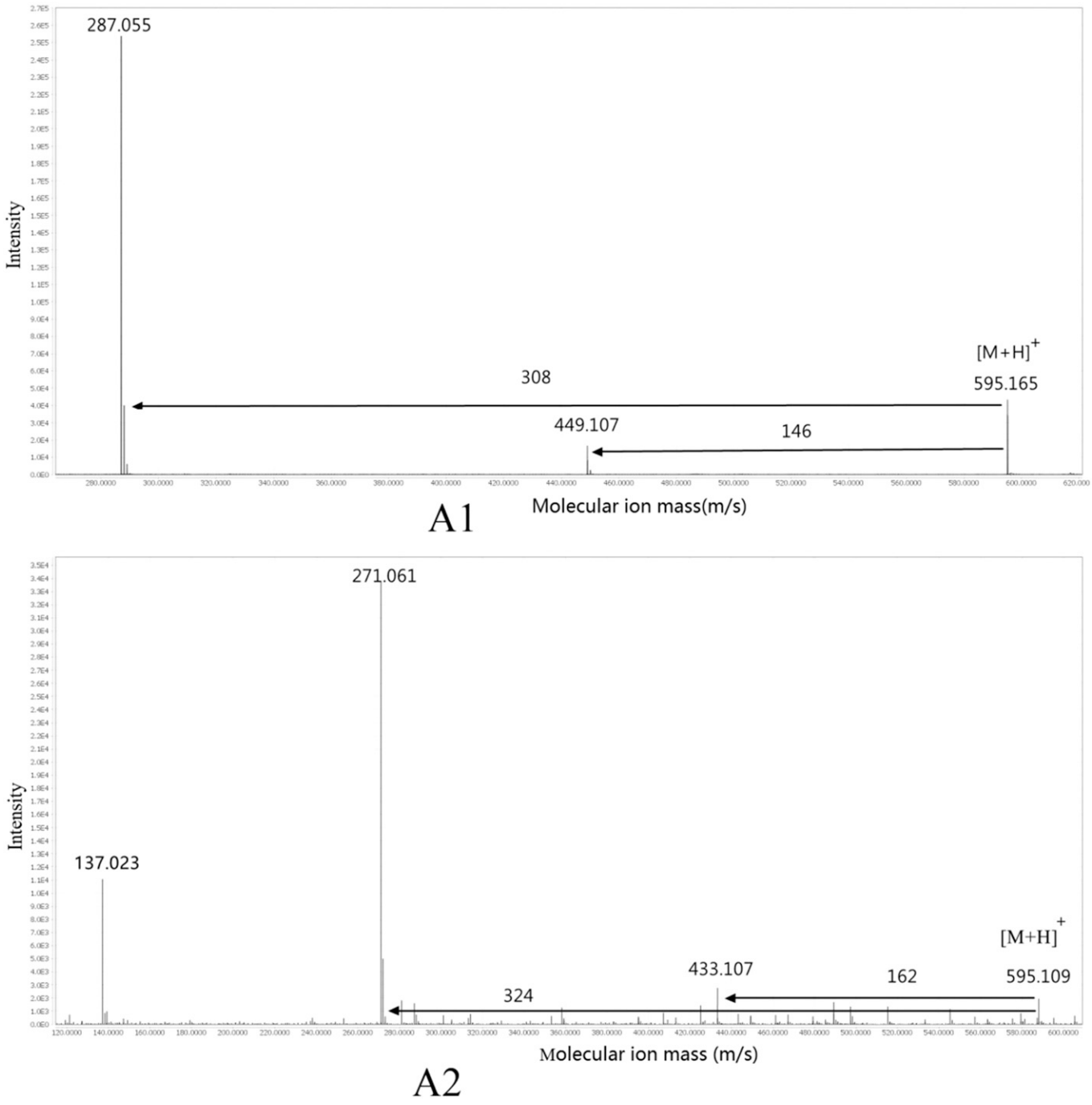

Supplemental Fig. 2. The mass spectra of anthocyanin A1, A2.

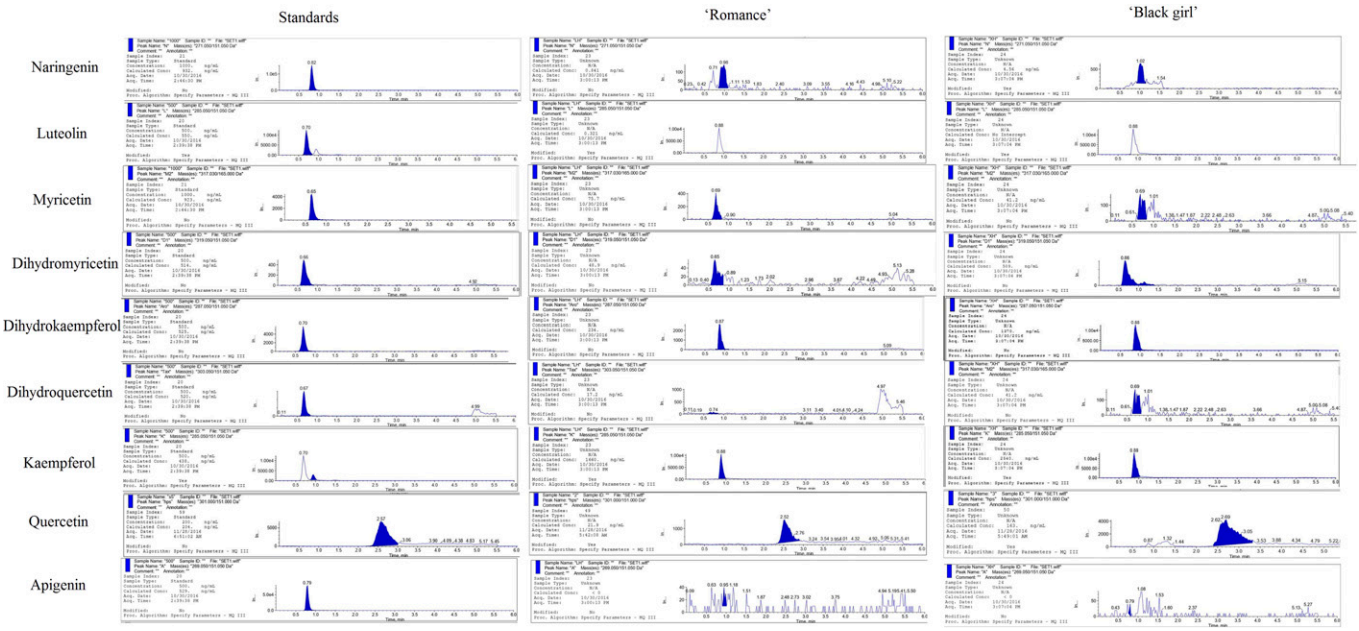

Supplemental Fig. 3. Ultra-performance liquid chromatography of flavones and flavonols in *Z. hybrida*.

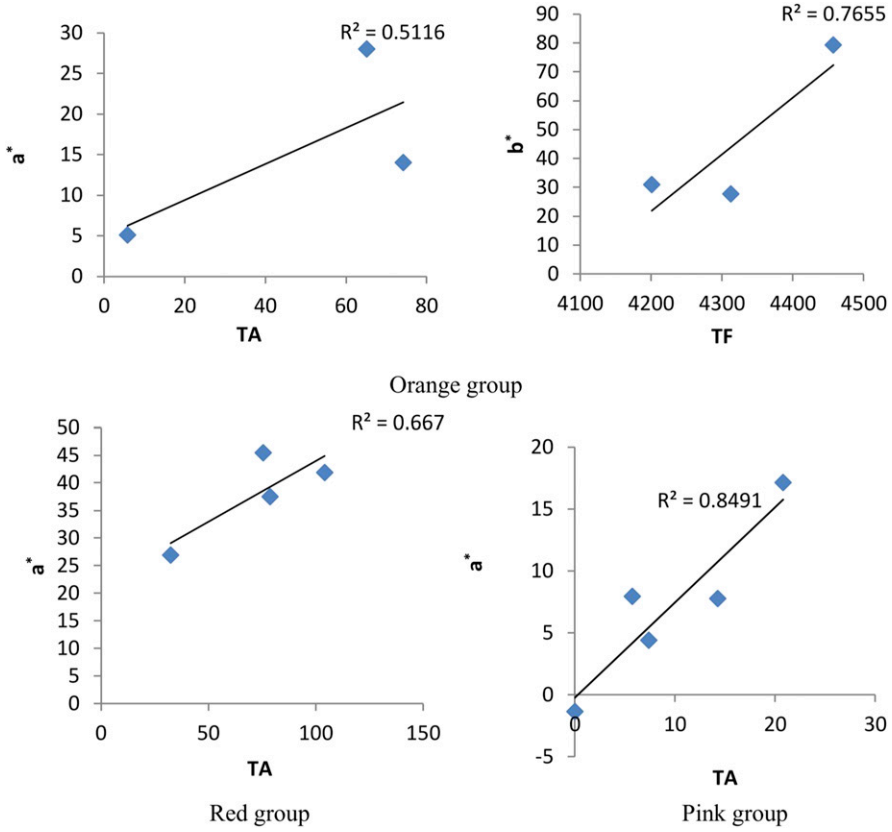

Supplemental Fig. 4. Relationships between redness (*a**) and total anthocyanin (TA) [or total flavones and flavonols (TF)] among of *Z. hybrida*.